Citation
Li, Z. and Chen, W. and Hao, H. 2018. Numerical study of open-top truncated pyramid folded structures with interconnected side walls against flatwise crushing. Thin-Walled Structures. 132: pp. 537-548. http://doi.org/10.1016/j.tws.2018.08.023

Numerical study of open-top truncated pyramid folded structures with interconnected side walls against flatwise crushing

Zhejian Li[1], Wensu Chen[1*], Hong Hao[1,2]*

[1]*Centre for Infrastructural Monitoring and Protection*
School of Civil and Mechanical Engineering, Curtin University, Australia
Kent Street, Bentley, WA 6102, Australia
[2]*School of Civil Engineering, Guangzhou University, China*

*corresponding author

Abstract

In this study, new types of folded structures with different base shapes (i.e. triangle, square and pentagon) are proposed. Each structure is folded from a thin sheet of aluminium, with the geometry of open-top truncated pyramid and connected inclination sidewalls. The purpose of this unique geometry is to increase the crushing resistance of the folded structure while maintaining a uniform collapsing behaviour under different crushing rates as compared with other existing folded kirigami structures. Three base shapes, i.e. triangle, square and pentagon, are considered in this study. Geometric parameters are derived for these structures based on three governing parameters: top and bottom edge length and cell height. Numerical models of these structures are firstly calibrated with quasi-static crushing test data followed by dynamic crushing simulations. To evaluate the crushing performances, structural responses including peak and average crushing stress, uniformity ratio and densification strain are compared among these three structures and also with the widely studied Miura-origami structure of the same density. Superior performances of crushing are observed for the proposed open-top truncated pyramid structure with higher average stress and more uniform collapsing under various loading rates, indicating potential application as energy absorber.

Keywords: Crushing; folded; kirigami structure; dynamic response; energy absorption**;** base shape

1. Introduction

One of the most widely known rigid foldable origami pattern was firstly proposed by Miura [1] in 1972. Miura-type origami structure is folded from an un-broken sheet material along straight creases without twisting or stretching the structure faces. It was firstly proposed as a solar panel packaging method for space deployment [2] and recently investigated as core of sandwich structure [3-5]. Comparing with conventional sandwich structure core such as honeycomb, the open channel design of Miura-type origami core allows moisture and heat to escape, as well as the ability to be continuously fabricated from one thin sheet material [5, 6]. In terms of crushing resistance, however, Miura-type origami core is not comparable to the conventional honeycomb core of similar density [7]. Furthermore, failure mode of plate buckling is also observed on Miura-type core under out-of-plane impact, leading to a non-uniform collapse. It also has a high initial peak force followed by a significant force reduction [5], a drawback for being used as a sacrificial layer for structure protection as the honeycomb core.

To increase the crushing resistance and achieve a more uniform crushing resistance of the folded structure, curved-crease foldcores were proposed [7, 8]. Different from the standard Miura-type foldcore, curved-crease foldcores are folded along curves instead of segments of straight lines. Good performance of this type of foldcore is shown by comparing with the standard Miura-type, with an increase in average crushing stress and a more uniform collapsing of the core. Its crushing resistance is also comparable with honeycomb structure of the same material and density while possessing a much more uniform collapsing [9]. Crushing behaviours of Kirigami foldcore have been recently studied as well [10]. Different from Origami foldcore, the sheet of kirigami structure can be cut, stamped or punched prior to folding, therefore achieving more complex geometry and potentially increasing their crushing resistance capacity. Up to 74% rise in average crushing stress is achieved for cube strip kirigami foldcore under quasi-static crushing comparing to the standard Miura-type origami foldcore and a comparable crushing resistance to honeycomb structure [10]. However, unlike other folded structures, the best performing kirigami structures including both cube strip and diamond strip kirigami foldcores, cannot be fabricated using a single sheet material. Multiple sheet strips are required to be folded individually and placed for the fabrication of a single panel.

In many of the existing kirigami folded structures [10, 11], not all vertical faces are connected with adjacent faces. Further improvements in crushing resistance and energy absorption are

expected for folded structure with connected vertical faces, due to more constraints provided under out-of-plane crushing. However, fully constrained cellular core could lead to a non-uniform collapsing with a high initial peak force and the crushing resistance may become very sensitive to strain rate due to the inertial stabilization provided by the fully connected sidewalls, similar to honeycomb structure [12]. An open-top truncated square pyramid folded structure (Figure 1) with interconnected sidewalls was proposed and studied in [13, 14], aiming to achieve a higher crushing resistance as well as single sheet fabrication. Its structural behaviours under out-of-plane quasi-static and dynamic crushing were investigated and compared with cube strip kirigami foldcore and aluminium foam of the same density. Good performances with high crushing resistance, low uniformity ratio (i.e. ratio of peak to average crushing stress), large densification strain and low strain rate sensitivity were observed for the proposed truncated square pyramid folded structure. Its blast mitigation capability as cladding core was also numerically studied [15, 16].

Figure 1. Sample of a single unit of truncated square pyramid folded from aluminium sheet （hand folded）

Open-top truncated pyramid kirigami foldcores with different base shapes including triangle, square and pentagon are experimentally and numerically studied in this paper. Three samples are named as truncated triangular pyramid (TTP), truncated square pyramid (TSP) and truncated pentagonal pyramid (TPP). Samples of these foldcores are folded by hand and crushed under quasi-static loading condition. The crushing test data is used for the construction and calibration of the numerical model. Dynamic out-of-plane crushing are then carried out numerically for these foldcores and compared with standard Miura-type foldcore of the same density and similar dimensions. The effects of geometric parameters of the truncated pyramid foldcore such as base shape, interconnection size and shape are investigated and discussed.

2. Geometric parameters

Table 1. Geometric parameters of three folded structures with base shapes of triangle, square and pentagon

	Truncated triangular pyramid (TTP)	**Truncated square pyramid (TSP)**	**Truncated pentagonal pyramid (TPP)**
c	$\sqrt{\left[\left(\frac{a-b}{2}\right)tan\frac{\pi}{6}\right]^2+H^2}$	$\sqrt{(\frac{a-b}{2})^2+H^2}$	$\sqrt{\left[\left(\frac{a-b}{2}\right)tan\frac{3\pi}{10}\right]^2+H^2}$
l	$\sqrt{\left(\frac{a-b}{2sin\pi/3}\right)^2+H^2}$	$\sqrt{(\frac{a-b}{2})^2+c^2}$	$\sqrt{\left(\frac{a-b}{2sin\pi/5}\right)^2+H^2}$
γ	$\arcsin\left(\frac{c}{l}\right)$	$\arctan\left(\frac{2c}{a-b}\right)$	$\arcsin\left(\frac{c}{l}\right)$
β	$\arcsin\left(\frac{H}{l}\right)$	$arcos\left(\frac{\sqrt{2}a-\sqrt{2}b}{2l}\right)$	$\arcsin\left(\frac{H}{l}\right)$
α	$\gamma-\frac{\pi}{6}$	$\gamma-\frac{\pi}{4}$	$\gamma-\frac{3\pi}{10}$
x	$\frac{sin\beta\cdot l}{sin(\pi-\alpha-\beta)}$	$\frac{sin\beta\cdot l}{sin(\pi-\alpha-\beta)}$	$\frac{sin\beta\cdot l}{sin(\pi-\alpha-\beta)}$
A_{surf}	$3\times\frac{1}{2}c(a+b)+6\times\frac{1}{2}sin\alpha\cdot xl$	$4\times\frac{1}{2}c(a+b)+8\times\frac{1}{2}sin\alpha\cdot xl$	$5\times\frac{1}{2}c(a+b)+10\times\frac{1}{2}sin\alpha\cdot xl$
ρ_v	$\frac{4A_{surf}\cdot t}{a^2tan\frac{\pi}{3}H}$	$\frac{A_{surf}t}{a^2H}$	$\frac{4A_{surf}\cdot t}{a^2\cdot\tan\frac{2\pi}{5}\cdot(2\cos\frac{2\pi}{5}+1)^2\cdot H}$

Folding configurations of three truncated pyramid kirigami structure are shown in Figure 2. As can be observed in Figure 1, small folding gaps near the corners of the unit cell may exist, which are considered in the numerical models. Triangular interconnections are placed to connect all adjacent inclined sidewalls along the vertical folding creases for each unit cell. Therefore, the geometry of the folded structure is governed by three parameters only, the length of bottom and top edges, *a, b* and the foldcore height *H*. Other geometric parameters (*c, l, α, β, γ, x*) marked out in Figure 2 can be expressed by three governing parameters *a, b* and *H* as shown in Table 1. Note that A_{surf} is the surface area of a single unit cell of the foldcore, ρ_v is

the volumetric density of the foldcore, and T is the thickness of the cell walls of foldcore. ρ_v is calculated using the volume of sheet material in one unit cell divided by the overall volume.

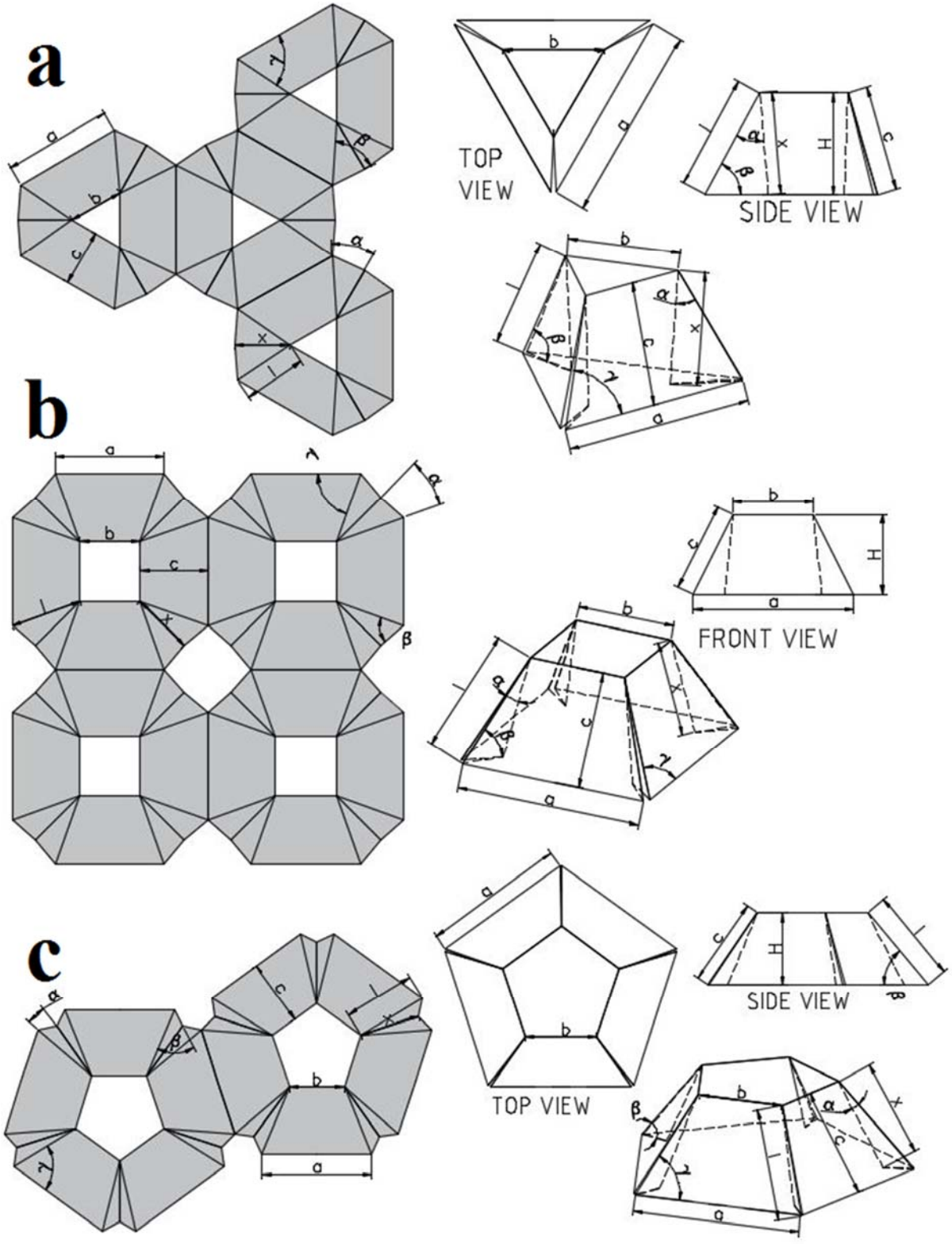

Figure 2. Folding creases and folding configurations with geometric parameters marked out for (a) truncated triangle, (b) square and (c) pentagon pyramid folded structures

In order to form a tessellated pattern using these structures, polygons on both top and bottom planes are set to be regular polygons in this study. In other words, sides of polygons are in equal length for individual unit cell of triangle, square and pentagon truncated pyramid structures. Tessellated pattern can be easily formed without any gap for triangle and square truncated pyramid kirigami structures. As for pentagon, there is no possible way to arrange them in a plane in order to form edge-to-edge contact with all adjacent ones. Different arrangements are studied where various patterns are formed with slight gaps between adjacent regular pentagons [17]. One of the simplest tessellated pattern for pentagon is used for this study as shown in Figure 3, where a single unit cell is marked out in dash lines including the pentagon and small gaps on both sides. Note that the base area used in calculation is the unit cell base area including the pentagon and the small gap marked out. This unit cell area selection is important for crushing behaviour of pentagonal truncated pyramid as sidewalls from adjacent units may slide towards and interact with each other. Boundary conditions for quasi-static test and numerical simulation are set accordingly.

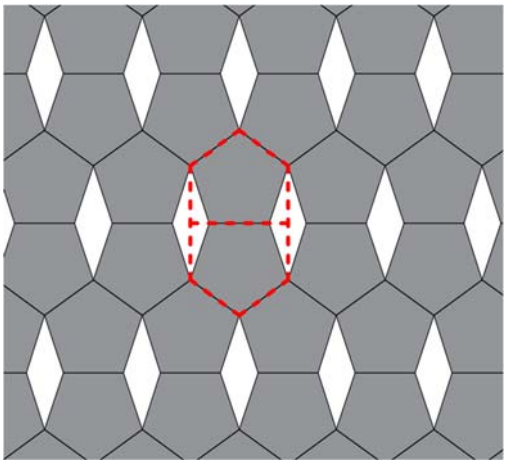

Figure 3, Simple tessellated pattern for regular pentagons where single unit cell area is marked out in dash lines

3. Numerical model validation

3.1 Quasi-static compression test

Hand-fold samples of three structures are crushed under quasi-static compression test with a constant rate of 1 mm/min, as shown in Figure 4. The three key governing parameters, bottom and top edge length, *a, b* and height *H* are kept same for all the three structures, where *a=40 mm, b=20 mm, H=20 mm*. Other parameters are shown in Table 2.Three samples have the same top and bottom edge length and height. It should be noted that 0.15 mm sheet for TTP and 0.26 mm sheet for TSP give the same relative density (or volumetric density) of 2.7% for testing.

Due to the availability of aluminium sheet in Australian market, there is no aluminium (1060) sheet with proper thickness for TPP to have the same relative density as TTP and TSP for the tests. In the tests, 0.26 mm sheet is used for TPP to give the volumetric density of 1.7%. In the subsequent numerical simulation, the thicknesses for TTP, TSP and TTP are adjusted as 0.15mm, 0.26mm and 0.43mm, respectively to ensure the same relative density of 2.7% and their performances are analyzed and compared.

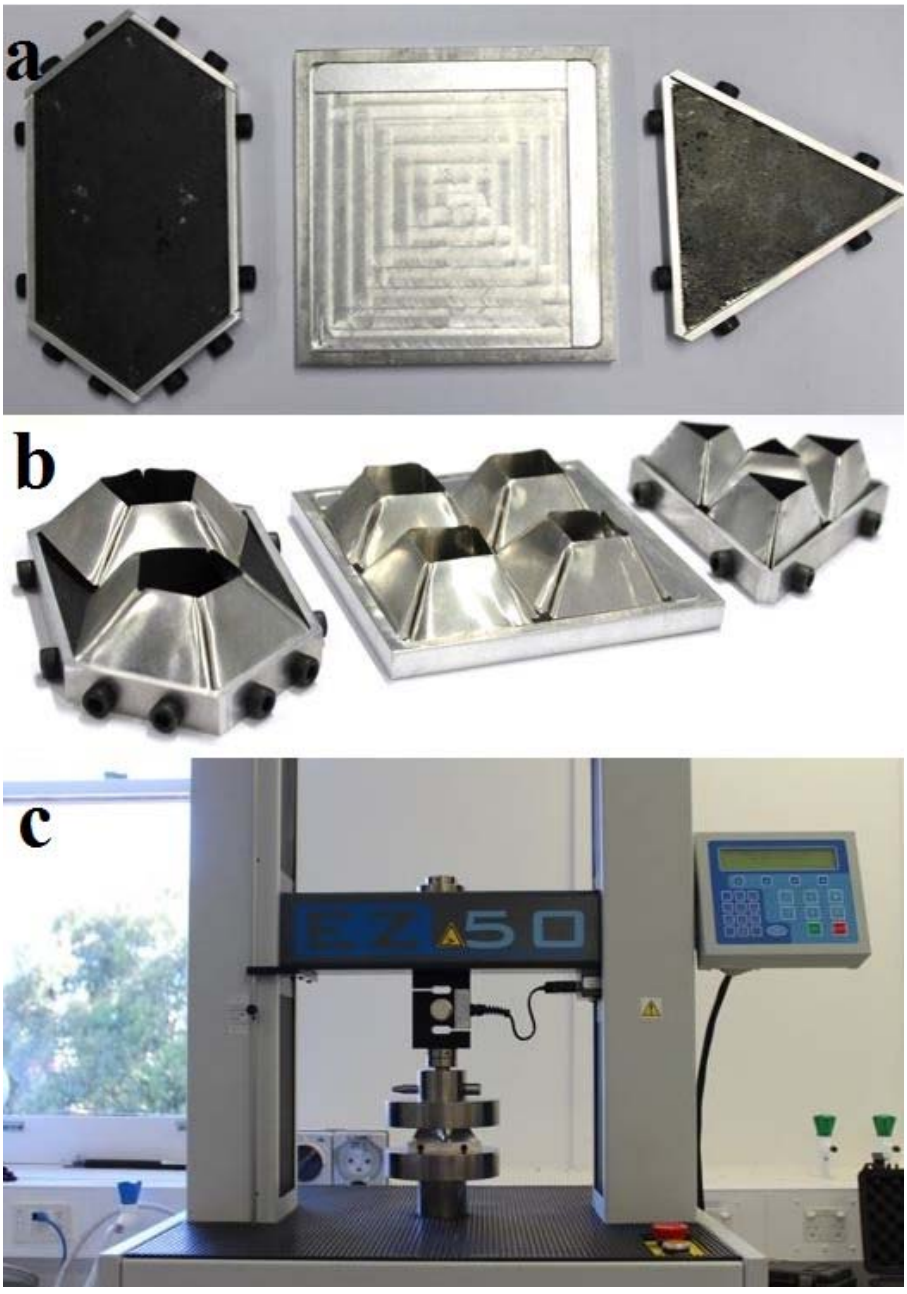

Figure 4. (a) Base plates of the foldcores with 2 mm high outer boundary; (b) foldcores set-up with base plates; (c) quasi-static crushing test set-up

Table 2. Geometric parameters of hand folded samples

Fold core	a (mm)	b (mm)	H (mm)	c (mm)	l (mm)	γ (degree)	β (degree)	α (degree)	x (mm)	t (mm)	ρ_v %
TTP	40	20	20	21	23	64	60	34	20	0.15	2.7
TSP	40	20	20	22	24	67	55	22	21	0.26	2.7
TPP	40	20	20	24	26	68	50	14	22	0.26	1.7

As shown in Figure 4 (b), some slightly bent sidewalls and minor gaps can be observed near the bottom edges, caused by hand folding process. These hand folding induced imperfections are unlikely to be avoided. Advanced machining such as stamping can be developed in future to reduce the imperfections and enhance folding speed. Samples are simply supported by a steel plate with the boundary of 2 mm high to constrain the sidewall movements along the bottom edges. This is to better investigate the behaviour of a foldcore with an array of unit cells where the interaction between adjacent sidewalls shall be considered. Glue and other types of fixing between foldcore and support plate are not used.

Tensile test of the aluminium sheet used for sample fabrication is carried out to obtain its stress strain data based on ASTM E8M-04 [18]. A constant loading rate of 0.5 mm/min is applied for the aluminium strip specimen with the thickness of 0.26 mm. The full fields of displacement and strain of the specimens are measured using Digital Image Correlation (DIC-2D) techniques. The DIC image of strain field along loading direction of aluminium strip specimen at maximum strain and the obtained true stress strain curve are shown in Figure 5.

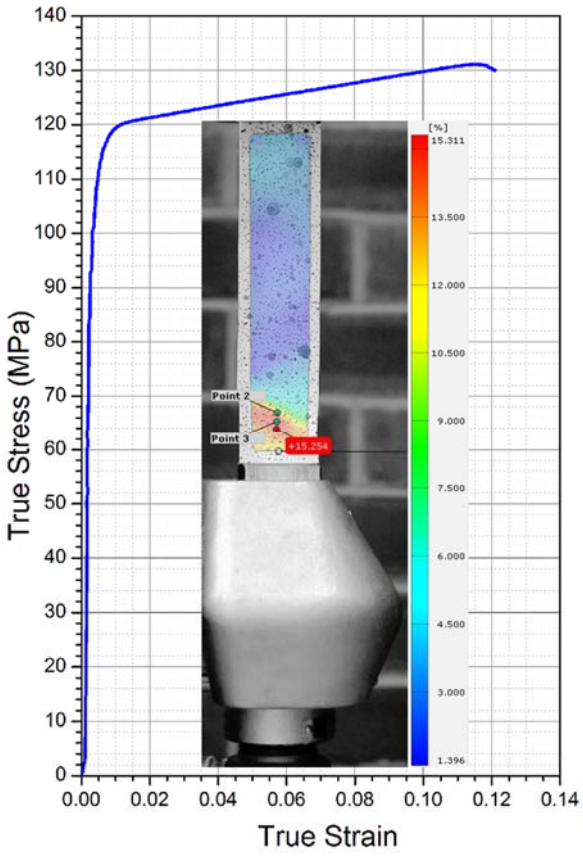

Figure 5. DIC image of aluminium strip specimen under direct tensile test at its maximum strain and true stress strain curve of aluminium 1060 strip tested

3.2 Numerical modelling

Finite element software LS-DYNA 971 is used for numerical simulation in this paper. The folded structures are constructed using Belytschko-Tsay type shell element and placed between two rigid solid blocks. The bottom solid block is set to be a fixed rigid block, and the top block moves at a constant speed of 0.05 m/s towards the fixed base plate till around 80% crushing strain is reached for the foldcores. The 1mm/min quasi-static crushing speed used in test is time consuming for the numerical simulation and 0.05 m/s was found sufficient to simulate accurate quasi-static loading in the numerical simulation [10]. Similar to the testing set up in Figure 4, simple boundary condition is applied for foldcore where the base plate has a 2mm high boundary and no glue or fixing is used in the numerical model as presented in Figure 6.

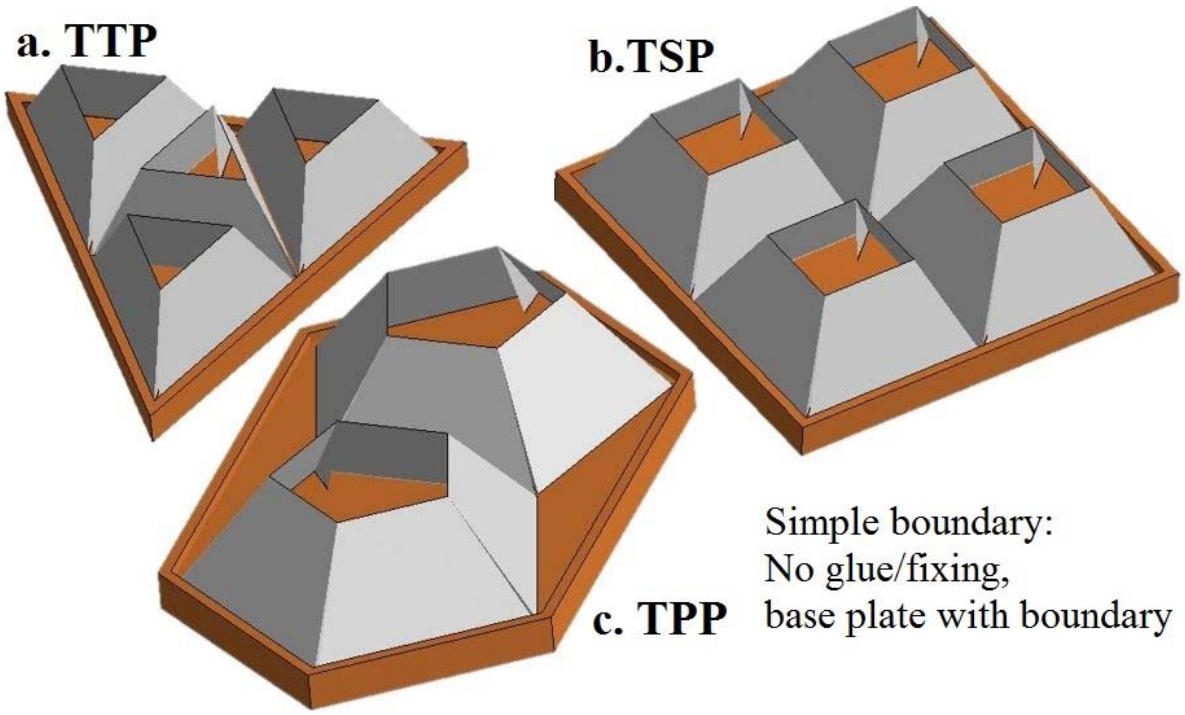

Figure 6. Numerical models of TTP, TSP and TPP folded structures with simple boundary

Material model *MAT024 PIECEWISE LINEAR PLASTICITY is used for the foldcore. Material properties and true plastic stress-strain data of aluminium 1060 sheet material are listed in Table 3 and Table 4. The strain rate effect of aluminium is not considered in this study, as it is not significant [19]. Contacts are described using keyword *CONTACT AUTOMATIC SINGLE SURFACE and *CONTACT AUTOMATIC NODES TO SURFACE for self-contact of the cell walls during the crushing process and the contact between foldcore and the support plate/top crushing plate, respectively. Friction is considered for both contacts.

Table 3. Material properties of Aluminium 1060

Parameter	**Young's modulus (GPa)**	**Poisson's ratio**	**Yield stress (MPa)**	**Density (kg/m^3)**
Value	69	0.33	66.7	2710

Table 4. True plastic stress-strain data of Aluminium 1060

Strain	0	0.002	0.005	0.013	0.063	0.121
Stress (MPa)	0	66.7	112.3	120.1	125.8	130.6

3.3 Model validation

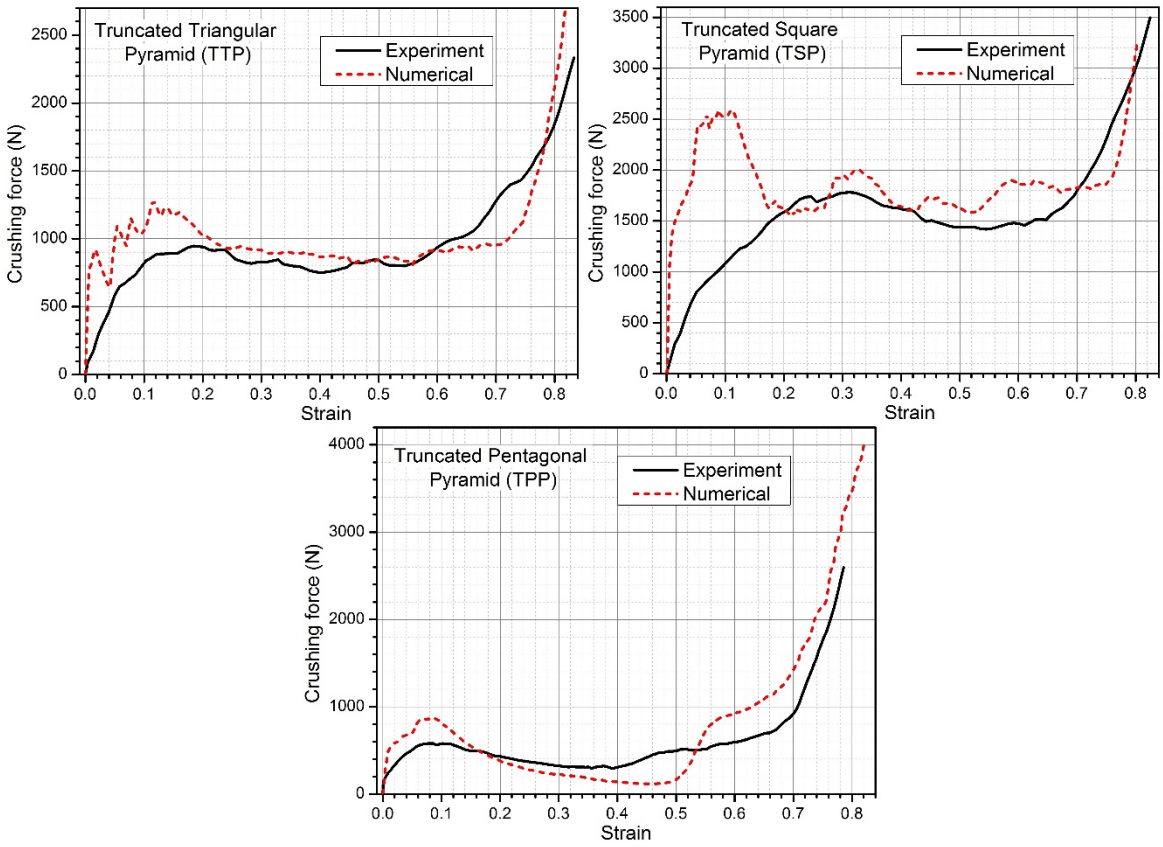

Figure 7. Comparison of stress-strain curves of three types of foldcores from numerical simulation and experimental tests

The stress-strain curves for the three types of truncated pyramid kirigami structures from both numerical simulation and quasi-static experiment are presented in Figure 7. Some discrepancies of initial peak crushing force are shown in all the three types of structures, which is caused by the imperfections of the samples induced by hand folding process. As can been seen from Figure 4 (b), the sidewalls are slightly bent and some gaps are shown between the foldcore and the base plate, which leads to uneven loading and easier buckling of some walls in the initial crushing stage. Similar discrepancy has been observed for other folded structures as well [10]. Once initial deformation occurs and the loading plate is in full contact with the core structure, the FE simulation and experimental results match well. The key parameters including initial peak crushing force, P_{peak}, average crushing force, P_{ave}, uniformity ratio, U, and densificaiton strain, ε_D, from both experiment and numerical simulation are compared and given in Table 5. The intial peak forces from FE results are larger than those from experiments because of the imperfection of the hand folded cores as explained above. However, other key parameters, including plateau stress and densification strain, are in good agreement for all

foldcores. These two parameters determine energy absorption capability of the core [10]. Therefore, the numerical models of these open-top truncated pyramid folded structures are considered acceptable for evaluating the foldcore behaviour and energy absorption.

Table 5. Key parameters from experiment and numerical simulation

Foldcore		P_{peak} (kN)	P_{ave} (kN)	$U = P_{peak}/P_{ave}$	ε_D
TTP	Exp	0.95	0.82	1.16	0.67
	FE	1.27	0.94	1.35	0.71
TSP	Exp	1.78	1.49	1.19	0.70
	FE	2.59	1.83	1.42	0.73
TPP	Exp	0.58	0.46	1.26	0.68
	FE	0.86	0.46	1.86	0.65

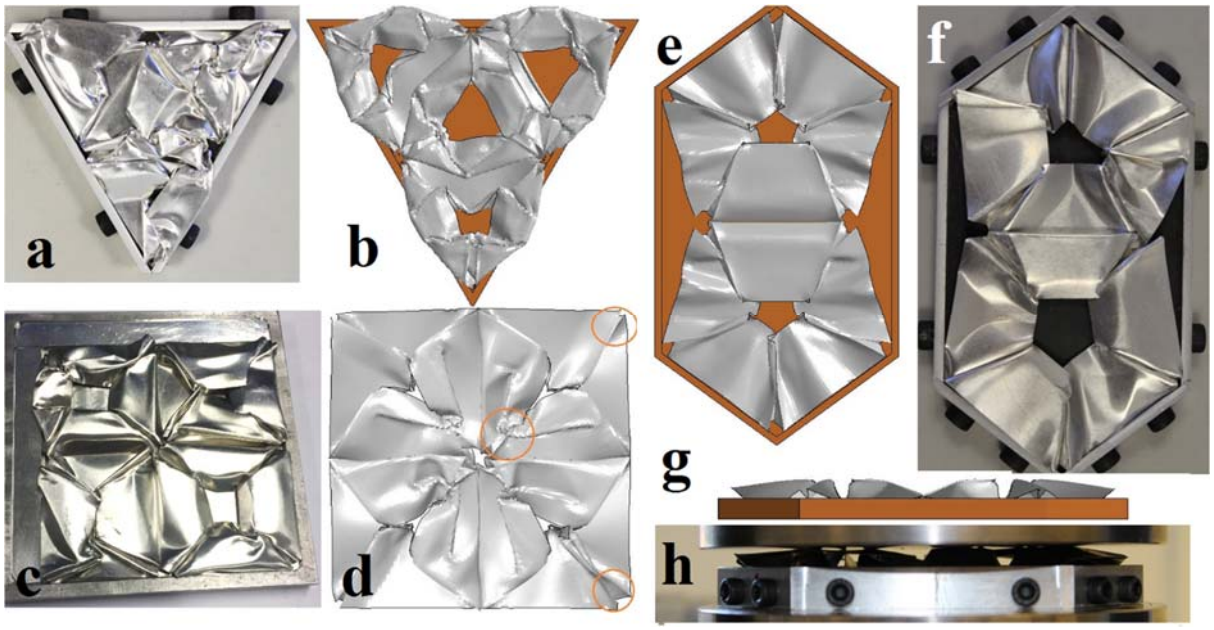

Figure 8. Damage modes (a) TTP experimental; (b) TTP numerical; (c) TSP experimental; (d) TSP numerical; (e) TPP numerical; (f) TPP experimental; (g) front view of TPP numerical; (h) front view of TPP experimental

Damage modes of the three types of folded structures are shown in Figure 8 by comparing both results from experimental test and numerical simulation. Due to the high inclination angle of TTP and TSP, multiple buckling on sidewalls especially along the intersection lines is presented. Deformations of these two types are less symmetrical and more randomly distributed in the experiment as compared to the numerical results. TPP, however, experiences less deformation on the sidewalls and no obvious buckling along intersection lines as the lines remain relatively straight. The sidewalls are bent towards centre of each unit cell and the lift-

up of the corners can be observed during crushing as shown in Figure 8 (g, h). The lift-up of corners is caused by the sliding in this simple boundary condition and the low inclination angle of TPP foldcore. The overall damage modes between experimental and numerical results are in good agreement.

4. Quasi-static crushing

Structural responses of three folded structures, i.e. TTP, TSP and TPP are numerically simulated and compared with the most common folded structure, i.e. Miura type origami [5]. The Miura type foldcore sample has the same overall dimensions as the truncated square pyramid (TSP), with the dimension of 80x80x20 mm and four unit cells. Other geometric parameters are shown in Figure 9. Same simple boundary condition is used for the numerical simulation as well as the material and contact settings. Because of the differences in geometries the tested samples have different relative densities. In numerical simulations, for comparison the relative density of all the considered core structures are made the same, i.e. 2.7%, which is achieved by adjusting the thickness of all foldcores including the Miura type. The corresponding parameters are listed in Table 6.

The wall thickness is calculated as: $t = \frac{\rho_v \cdot A_{base} \cdot H}{A_{surf}}$ where t is the wall thickness, ρ_v is the volumetric relative density, A_{base} is the base area of the model, H is the height of foldcore and A_{surf} is the outer surface area of the model.

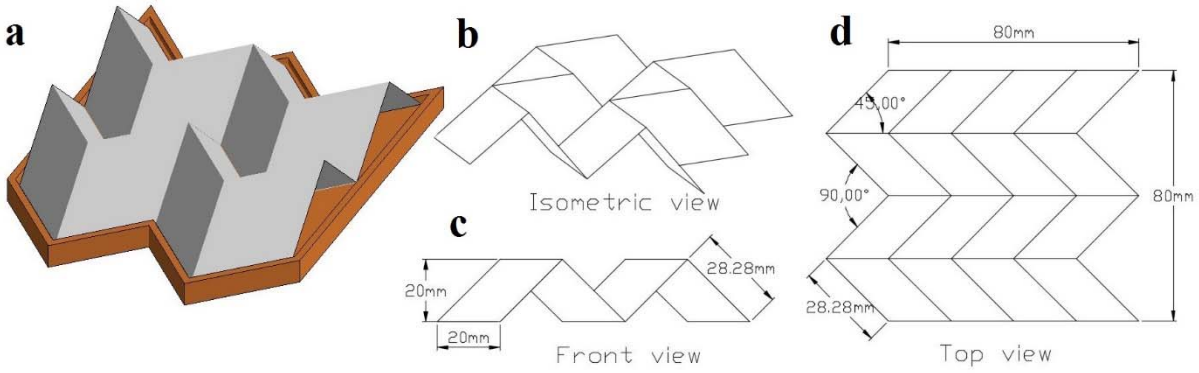

Figure 9. Miura-type origami foldcore with four unit cells (a) numerical model and base plate; (b) isometric view; (c) front view; (d) top view

Table 6. Parameters of the foldcores

Foldcore with relative density 2.7%	Miura type foldcore	Truncated triangular pyramid (TTP)	Truncated square pyramid (TSP)	Truncated pentagonal pyramid (TPP)

Wall thickness (mm)	0.31	0.15	0.26	0.43
model base area (mm^2)	6400 (4 unit cell)	2771 (4 unit cell)	6400 (4 unit cell)	6449 (2 unit cell)
model surface area (mm^2)	11081	10207	13337	8539

4.1 Stress-strain curve comparison among foldcores with simple boundary

The stress strain curves of these simply supported foldcores under quasi-static loading are presented in Figure 10. Truncated triangular pyramid (TTP) structure demonstrates the best performance among the considered foldcores. It has a lower initial peak stress, a higher average stress and larger densification strain comparing with the other truncated pyramid structures and the Miura-type foldcore. All the three types of truncated pyramid structures have a low initial peak stress resistances of truncated pyramid structures reach their overall peak at around 0.1 strain in indicating relatively low crushing resistance at early stage as compared to Miura-type foldcore. The crushing the plateau stage of the crushing as compared to the initial elastic stage for Miura-type which reaches its overall peak at around 0.02 strain. The average crushing stress of TTP and TSP exceed the Miura-type foldcore and possess a larger densification strain, which corresponds to a sudden increase of the stress-strain gradient at the end of the plateau stage of the deformation. As for TPP, the average crushing resistance is slightly lower than the other types and it has a similar densification strain as Miura-type, even though it has the lowest overall peak stress among these foldcores.

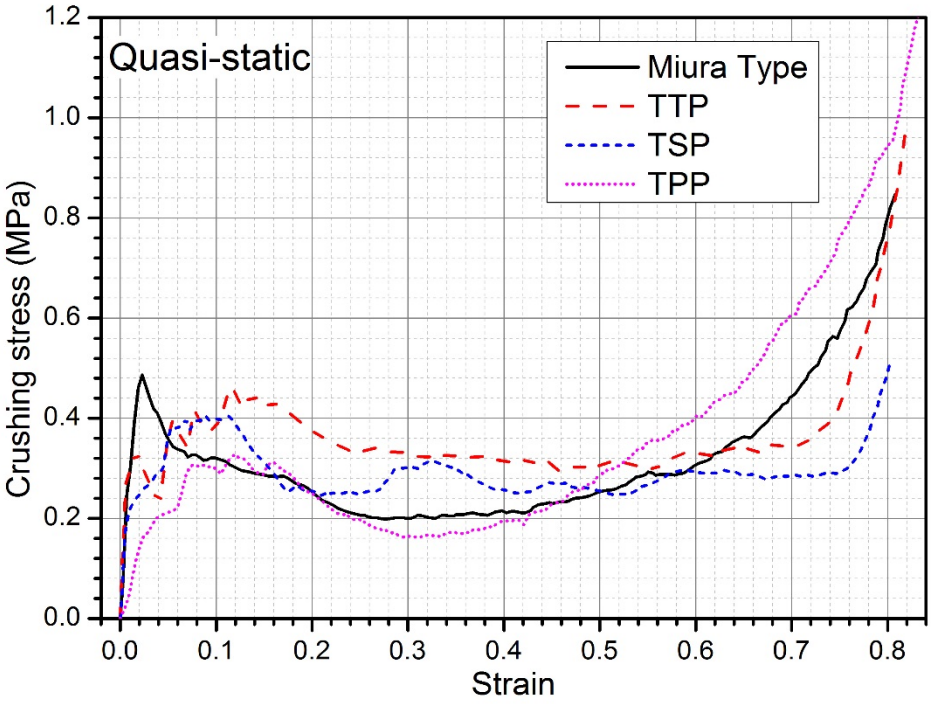

Figure 10. Stress strain curves of four types of foldcores under flatwise quasi-static crushing with simple boundary

Table 7. Peak and average stress, uniformity ratio (U) and densification strain (ε_D) of four foldcores under flatwise quasi-static crushing

Foldcore	σ_{peak} (MPa)	σ_{ave} (MPa)	U= σ_{peak} /σ_{ave}	ε_D
Miura	0.486	0.268	1.81	0.66
TTP	0.458	0.340	1.35	0.74
TSP	0.405	0.286	1.42	0.76
TPP	0.326	0.262	1.24	0.66

As listed in Table 7, the criteria used to evaluate crushing performance of the foldcores include peak and average stress, uniformity ratio which is the ratio between the peak and average stress, and densification strain. Both TTP and TSP have superior performance comparing to Miura-type foldcore in all four criteria, with higher average crushing resistance, lower initial peak stress, lower uniformity ratio and larger densification strain. Out of these four configurations of folded structures, TTP folded structure has the highest average crushing stress at 0.34MPa, around 27% higher than the standard Miura-type foldcore and 12% higher densification strain as well. This suggests an enhanced performance in terms of energy absorption capability. As concluded in a previous study [20], more corners could lead to higher crushing resistance and energy absorption capability. In the current study, the decreasing trend of plateau stress from TTP to TSP to TPP under this loading condition may be also attributed to the decreasing

number of folds per unit area, since TTP (12 folds/2770mm^2) has more folds per unit area than TSP (16 folds/6400mm^2) and TPP (10 folds/6449mm^2).

Furthermore, all truncated pyramid folded structures have a delayed peak stress at around 0.1 strain comparing with 0.02 strain for Miura-type as shown in Figure 10. Delayed peak stress with lower value indicates that the deformation is more consistent and easier to initiate at early stage for the proposed foldcores, which is another advantage of energy absorber.

4.2 Damage mode of foldcores with simple boundary

Damage modes of the foldcores at different strains under quasi-static crushing are shown in Figure 11. Different damage modes can be observed for the foldcores. For the widely studied Miura-type, the faces start to buckle along horizontal directions around the middle of the foldcore faces, which is followed by the sequential folding of faces along the buckling line at middle of the faces under further crushing. As shown in Figure 11 (a), sequential folding of the foldcore faces along the buckling creases can be observed with the increasing strain. This initial sheet buckling failure mode leads to a sharp increase in the crushing resistance followed by the sudden drop of the resistance. This failure mode is in good agreement with the previous studies of Miura-type foldcore [5, 21].

For the three types of truncated pyramid structures, the damage modes vary as well, because of the differences in inclination angle, the interconnection size and shape. For TTP structure, bending of the top edges of sidewalls towards unit cell centre can be observed at the strain of 0.2. Local buckling can be observed near the top corners at the interconnections, which is different from the Miura-type foldcore where the buckling occurs horizontally at the middle of foldcore face. For TSP foldcore, some faces have the similar deformation modes as TTP with top edge sidewalls bending inward and occurrence of local buckling along the corners. Other faces, however, have no local buckling along the interconnections, because of the reduction in inclination angle of the sidewall comparing to TTP. As can be seen from those circled in *Figure 11* (c), some intersection lines at corners are straight and some are buckled at 0.6 strain. Lift-up of the outer corners can also be observed. The predicted deformation of TSP is also symmetrical whereas in experiment is more randomly distributed. As for TPP, no buckling along the corner of unit cell can be observed, only sidewall faces vertically bend toward centre. As shown in circles, almost all corner edges of the TPP foldcore still remain straight at the strain of 0.6.

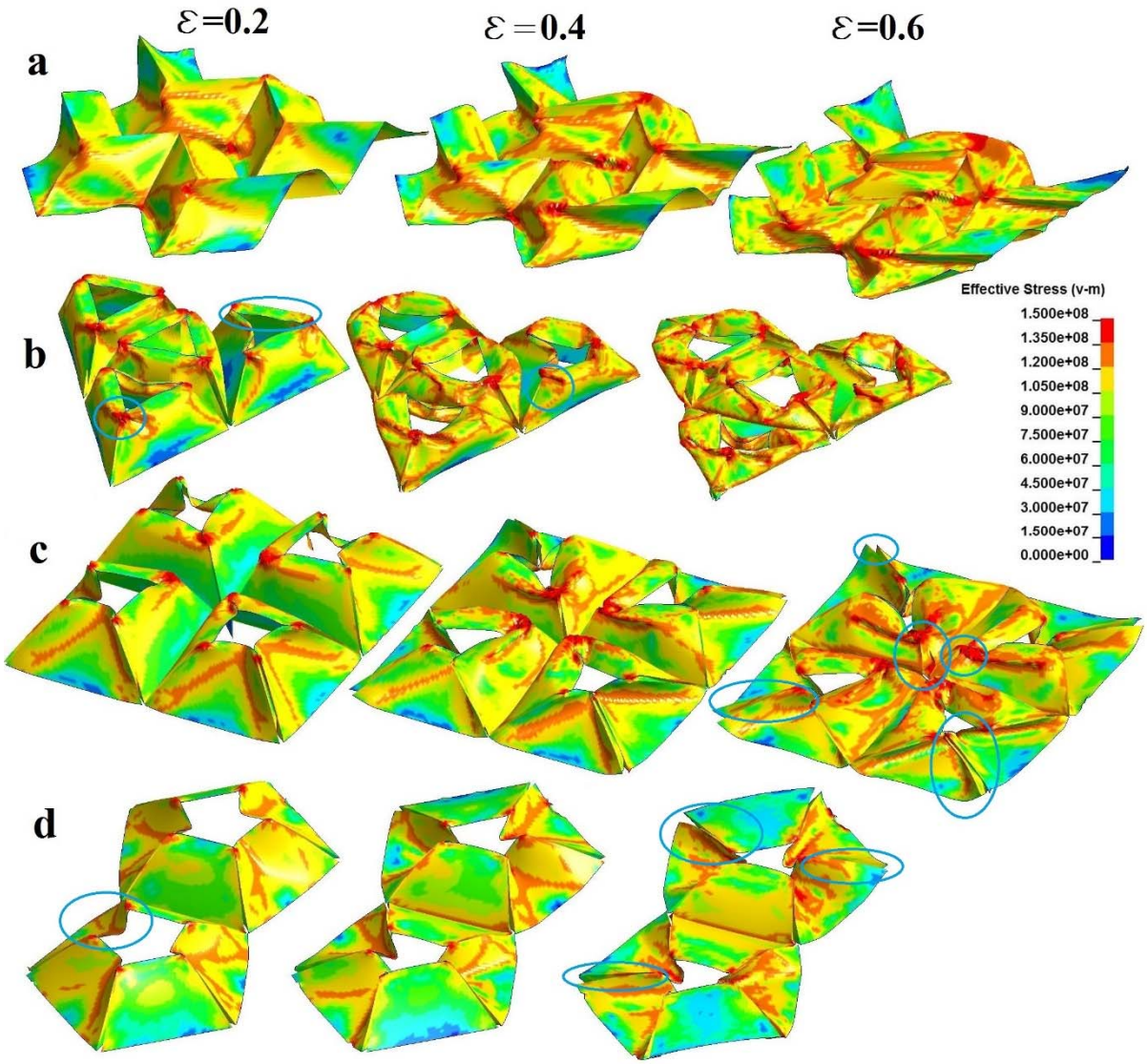

Figure 11. Damage modes of the foldcores with simple boundary at the strain of 0.2, 0.4 and 0.6; (a) Miura-type; (b) Truncated Triangular Pyramid; (c) Truncated Square Pyramid; (d) Truncated Pentagonal Pyramid

As investigated in the previous study [14], this initial top edge inward bending leads to low initial crushing resistance of the truncated square pyramid foldcore, which is followed by deformation of the sidewall buckling corresponding to the peak stress under crushing. Since the inward bending on top edges occurs prior to sidewall buckling for the proposed truncated structures, their initial peak stress are much lower than Miura foldcore. For TPP without experiencing any sidewall buckling near the unit cell corners, the average crushing resistance is much lower than the other two types. This is due to the lower inclination angle of sidewalls on TPP which leads to sidewall sliding and corner lift-ups under lateral crushing. Furthermore, the triangular interconnection size decreases with the increasing number of the sides, i.e., the size of vertical triangular interconnections which provide extra crushing resistance reduces

from TTP to TSP to TPP. This is consistent with the stress-strain curves of the foldcores as well.

4.3 Fixed boundary condition

Corner lift-up can be observed for TPP foldcore due to the non-ideal simple boundary condition, which leads to different damage modes and lower crushing resistance comparing to TTP foldcore. Different boundary conditions are therefore studied to exam its effect on structural behaviour. The bottom outer edges of the foldcore unit area are fixed in both the in-plane directions, while other parameters are kept the same. In other words, instead of modelling the base plate with 2 mm boundary (Figure 6), where sliding of the sidewalls might occur, the foldcore outer bottom edges are now fixed with no displacement allowed. This is to simulate one of the most common connection of sandwich core to its skin, where glue or fully fixed connection is often used. For the folded structure, this fixed boundary condition may be also achievable by using grooved base plate as shown in Figure 12 (a), which was used as the testing base plate for an origami-tube [22]. Deformation and crushing resistance of the foldcores are investigated under the fixed boundary condition.

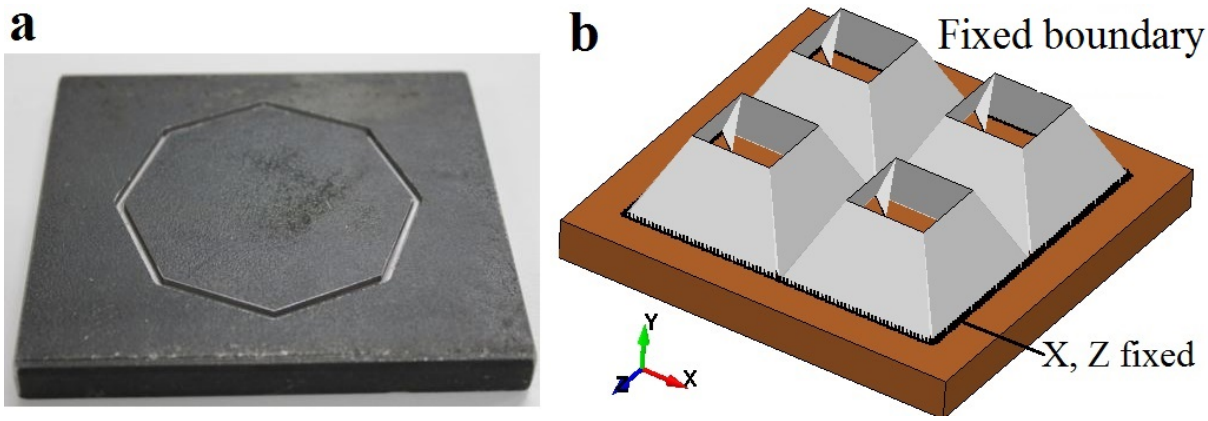

Figure 12. (a) Grooved base plate for origami-tube crushing test [22]; (b) Fixed boundary with outer edges of foldcore fully fixed along the in-plane directions

The numerical results of engineering stress-strain curves for these foldcores with fixed boundary under quasi-static loading are shown in Figure 13. Similar crushing behaviours are shown for Miura-type and TPP foldcore as those obtained above with simple boundary condition as shown in Figure 10. Miura-type foldcore experiences higher initial peak stress with a slightly shorter elastic stage, where the peak stress is achieved earlier than the case with simple boundary condition. Other than this, the stress-strain response including the average stress and densification strain remains similar for the cases with the two different boundary

conditions. For the other two types of truncated pyramid foldcores, i.e., TSP and TPP, distinct discrepancy of structural response can be observed from the strain of 0.2 onwards, as compared to the case with simple boundary condition. Although the structural response seems similar at the early stage of the crushing for the both boundary conditions, both foldcores of TSP and TPP show significant increase in the average crushing resistance during the plateau stage of crushing when the boundary of the foldcores is fixed.

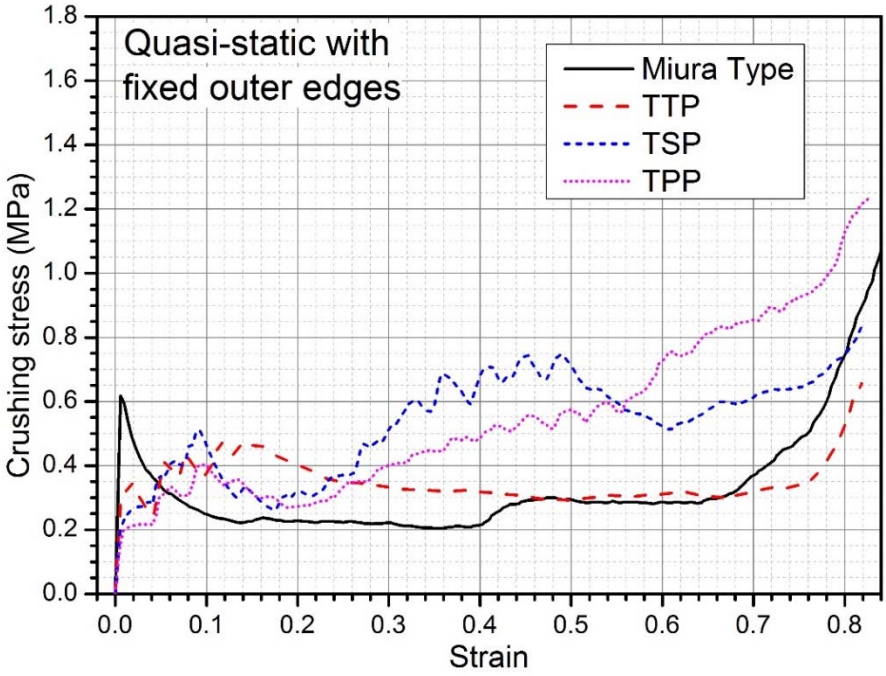

Figure 13. Stress strain curves of four types of foldcores with fixed outer edges under flatwise quasi-static crushing with fixed boundary condition

This increased resistance is caused by the change of deformation mode of these two types of foldcores (TSP and TPP) under fixed boundary. The damage modes of foldcore under this boundary condition at the strain of 0.4 are shown in Figure 14. Consistent with the stress-strain curves, the damage modes of the Miura-type and TTP foldcore under fixed boundary are similar to the case with simple boundary condition as shown in Figure 11 (a, b). The Miura-type foldcore has similar buckling failure occurred at the middle of the faces on foldcore along the horizontal direction for two boundary conditions. Similar damage mode for TTP foldcore with the two boundary conditions is also observed. Top edges of the foldcore bend slightly toward centre of each unit cell and obvious buckling can be observed along the interconnection lines of the sidewalls.

Significant differences in the deformation mode of TSP and TPP foldcores are shown for two boundary conditions. As shown in Figure 11 (c) with simple boundary, some sidewalls of TSP

foldcore are bent vertically towards centre and no deformation is presented along the outer intersection lines, other faces and interconnections are buckled near the intersection lines. For TPP foldcore with simple boundary condition shown in Figure 11 (d), only vertical bending of sidewalls towards centre is presented, all the intersection lines between faces of foldcore remain straight and un-deformed. Under fixed boundary condition, however, as shown in Figure 14, TSP and TPP foldcores deform similarly, with rolling of the top edges towards centre, and buckling along top of the intersection lines. No lift-up or deformation of foldcore corners at bottom is shown. The change of deformation mode is correlated to the change of crushing resistance under the two boundary conditions for TSP and TPP folded structures. The vertical bending of sidewalls towards the centre, shown in simply supported scenario, requires less force. With simple boundary, faces are free to slide causing corners to lift-up. The foldcore with lower inclination angle is easier to initiate the sliding of sidewalls due to the larger force in horizontal direction. Therefore, the foldcore with low inclination angle such as TSP and TTP is prone to experience the sliding and corner lift-up as shown in Figure 8 (g,h) and Figure 11 (c,d). With fixed boundary, sliding of the sidewalls and the corner lift-ups are minimized, and the buckling deformation occurs along the triangular interconnections between sidewalls rather than vertical bending of sidewalls. Therefore, with fixed boundary, the crushing resistance capacity is enhanced for TSP and TPP foldcores which have lower sidewall inclination angle.

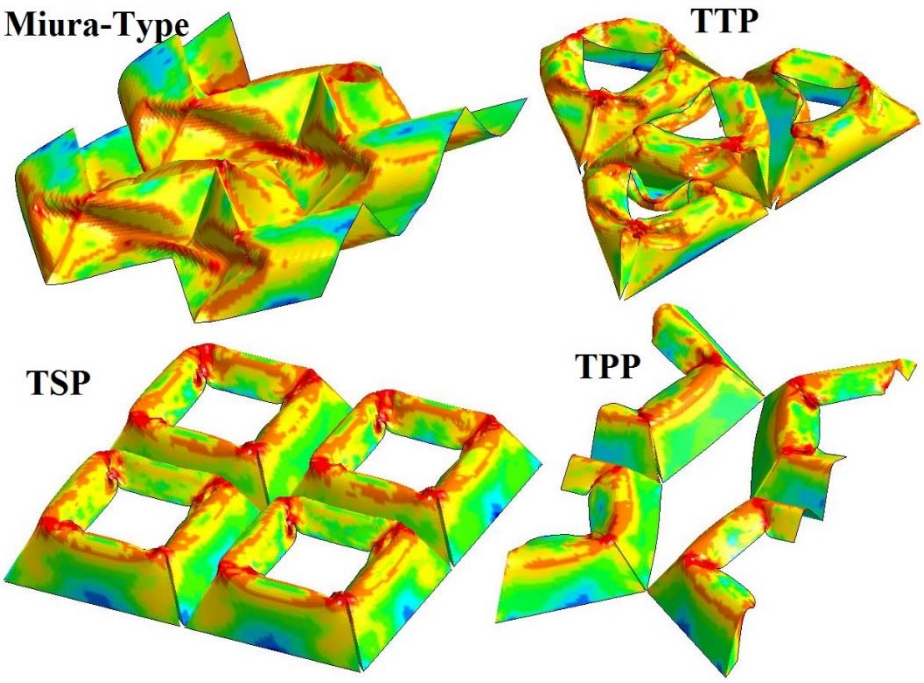

Figure 14. Damage modes of the foldcores at the strain of 0.4 with fixed boundary; Note: symmetric model used for TPP to simulate the interaction of adjacent unit cell at the gap

5. Simple boundary dynamic crushing

5.1 Stress-strain curve comparison under dynamic loading

In this section, structural behaviours of the foldcores are studied under different crushing velocities. The foldcores have the same unit number with simple boundary condition as in quasi-static testing where foldcore are simply supported by the same base plate with a 2 mm high outer boundary. Stress-strain curves of these foldcores under dynamic crushing speeds of 0.05, 0.5, 5, 10 and 20 m/s are presented in Figure 15. Key criteria of these foldcore are listed in Table 8.

The initial peak stress of Miura-type foldcore is greatly affected by crushing speed. It increases almost three times from 0.486 to 1.906 MPa with crushing rate increasing from 0.05 to 20 m/s as shown in Figure 15. Similar drastic increase can be found for its uniformity ratio as well from 1.81 to 4.25, while the densification strain of Miura-type foldcore is only slightly affected by the crushing velocity. The Miura-type folded structure shows great strain rate sensitivity on its initial peak stress.

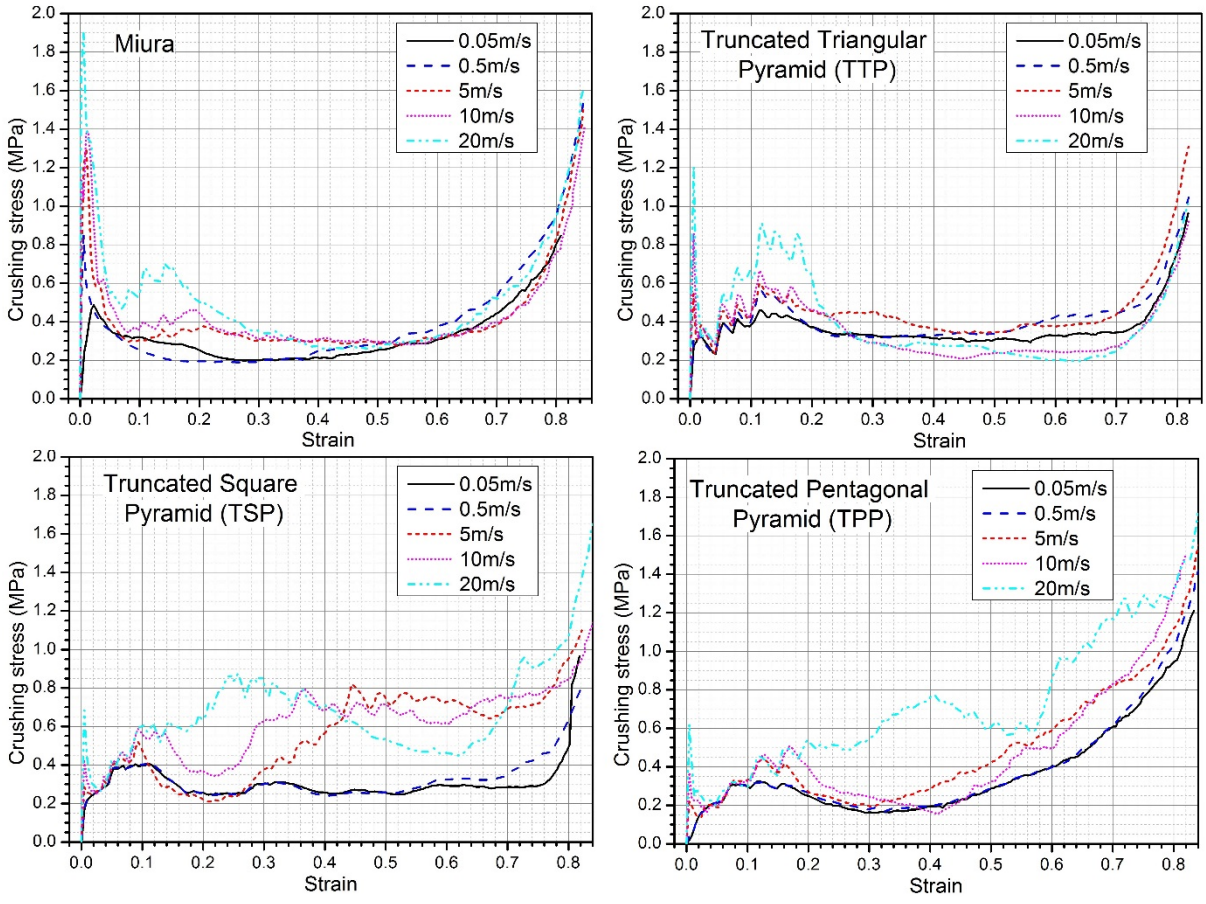

Figure 15. Stress-strain curves of foldcores under flatwise dynamic crushing with simple boundary

For the truncated pyramid folded structure, strain rate effect is dependent on the base shape and the geometry of the foldcore. Different dynamic behaviours with increasing crushing speed are observed for TTP, TSP and TPP as shown in Figure 15. For TTP folded structure, the increase in initial peak stress is obvious, from less than 0.4 MPa to 1.2 MPa, even though the increase is not as drastic as Miura-type foldcore. The average crushing stress of TTP structure, however, remain similar in value irrespective of the crushing velocity. For TSP folded structure, crushing behaviour remains almost unchanged under low speed crushing (0.5m/s). The initial peak stress has a much smaller increase under the crushing speed of 20 m/s comparing with Miura-type and TTP folded structure. The crushing behaviour, on the other hand, is greatly changed under higher crushing speeds (e.g. 5, 10 and 20 m/s). Significant increase in average crushing resistance and some reductions in densification strain can be observed in Figure 15. Similar trend of change in structural behaviour is shown for TPP folded structure with the increasing crushing speed as well. These crushing behaviours corresponding to the high crushing speed are somewhat similar to the quasi-static crushing case of the foldcores with the fixed boundary as shown in Figure 13. This is because the change of the crushing behaviour related to strain rate is caused by the change in damage modes, similar to the case associated with changing boundary conditions. More detailed discussions are given in section 5.2.

Table 8. Peak and average stress, uniformity ratio and densification strain of four foldcores under flatwise dynamic crushing

Foldcore type	Crushing speed (m/s)	σ_{peak} (MPa)	σ_{ave} (MPa)	$U= \sigma_{peak}/\sigma_{ave}$	ε_D
Miura	**0.05**	0.486	0.268	1.81	0.66
	0.5	0.847	0.283	2.99	0.67
	5	1.300	0.348	3.74	0.70
	10	1.384	0.382	3.62	0.70
	20	1.906	0.448	4.25	0.66
TTP	**0.05**	0.458	0.340	1.35	0.74
	0.5	0.559	0.380	1.47	0.75
	5	0.599	0.410	1.46	0.72
	10	0.859	0.331	2.60	0.73
	20	1.205	0.377	3.20	0.73
TSP	**0.05**	0.405	0.286	1.42	0.76
	0.5	0.409	0.297	1.38	0.72
	5	0.819	0.521	1.57	0.76
	10	0.792	0.604	1.31	0.80
	20	0.877	0.599	1.46	0.67
TPP	**0.05**	0.326	0.262	1.24	0.66
	0.5	0.324	0.271	1.20	0.66
	5	0.436	0.357	1.22	0.66

10	0.462	0.338	1.37	0.66
20	0.775	0.532	1.46	0.58

Overall, strong strain rate sensitivity is demonstrated for Miura-type foldcore with huge increase in the initial peak stress, which is non-ideal for some sandwich panel applications such as cladding or impact attenuator. The truncated structures are much less strain rate dependent owing to their geometries. The TTP folded structure with high inclination angle also shows a dependent crushing behaviour with strain rate, as the initial peak stress increases with the crushing speed, but at a less level as compared to that of Miura-type foldcore. For TSP and TPP folded structures, the initial peak stress is not significantly affected by the strain rate. The average crushing stress or plateau stress, however, increases with crushing speed due to the change of deformation mode. Their dynamic crush behaviour with the simple boundary condition is similar to the case with fixed boundary condition under quasi-static crushing. The increase of plateau stress under higher crushing speed could lead to a superior energy absorption capability, since with the same crushing distance the foldcore would absorb more energy without inducing a significant increase in initial peak stress.

5.2 Damage mode comparisons

The effective stress contour plot of Miura-type foldcore under 20m/s crushing is shown in Figure 16, the same legend is used as in Figure 11. Distinct deformation mode of the foldcore with simple boundary condition under dynamic loading is observed as compared to the case with simple boundary condition under quasi-static crushing shown in Figure 11. The plate buckling location shifts up to near the top of the foldcore instead of at around the middle of foldcore faces when crushing at a higher speed. Deformation along the bottom edges of the Miura-foldcore is less significant than quasi-static scenario, less rising of corners can also be observed under dynamic scenario. Similar dynamic behaviour of Miura-type foldcore has been identified in the previous studies as well [5, 23].The buckling location shifted closer to impact end and initial peak stress increased dramatically, which was explained by the inertia force developed inside the core under dynamic crushing [23]. The sharp rise of initial peak stress might be related to the constraints provided by the faces of adjacent rows as well. At a lower crushing speed, the buckling location is around the middle faces of the foldcore, at some distance to the intersection of faces from adjacent row. Therefore, with the buckling location shifting up, closer to the intersection line of adjacent row, larger inertia stabilization is provided by the adjacent faces, causing significant increase in initial crushing resistance. This inertia

stabilization effect is similar to the perpendicular webs of square honeycomb where sharp rises of initial crushing resistance are also observed under higher loading rate [12, 24].

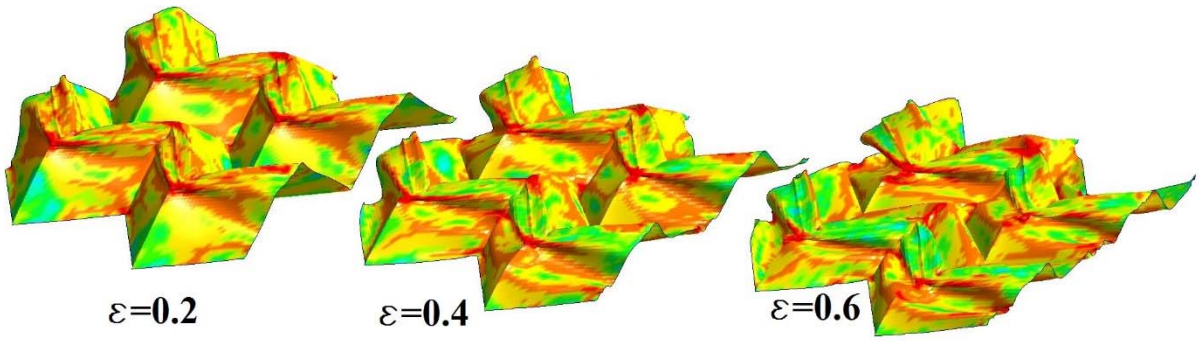

Figure 16. Damage modes of Miura-type foldcore at the strain of 0.2, 0.4 and 0.6 under 20m/s crushing with simple boundary

As shown in Figure 17, the damage mode of TTP folded structure with simple boundary under dynamic crushing is similar to that with simple boundary under quasi-static crushing as shown in Figure 11 (b). The top edge rolling towards unit cell centre and the buckling along the interconnections of sidewalls are observed. The sidewall buckling direction, however, shifts from bending towards outsides to inwards buckling. This is caused by the slight shifting up of the top edge bending location and the changed deformation modes. The high inclination angle of the sidewall of TTP unit cell leads to the increasing resistance to initial rolling on the top edge. Furthermore, due to the larger size of the vertical triangular interconnections as shown in Figure 2, the initial inertia effect is stronger for TTP than TSP and TPP which have smaller interconnections. Therefore, a sharp increase of initial peak stress occurs for TTP under dynamic loading as compared with the other two types of truncated pyramid structures. As previously studied [14], similar sharp rise in initial peak stress with the increasing crushing speed is observed for TSP foldcore with different geometric parameters (e.g. higher inclination angle and larger interconnection size) than the TSP with the geometry used in this study.

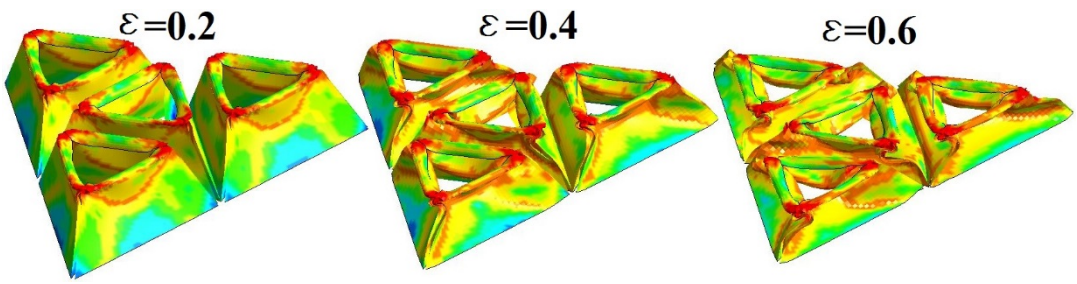

Figure 17. Damage modes of TTP folded structure with simple boundary at the strain of 0.2, 0.4 and 0.6 under 20m/s crushing

The deformation of the TSP folded structure is similar to the TTP foldcore under dynamic loading, as shown in Figure 18. Structural behaviour of TSP folded structure with simple boundary, however, shows distinct change under dynamic crushing as compared to the case under quasi-static loading. The deformation of vertical sidewall bending, which occurs on some faces of TSP foldcore unit cell under quasi-static loading, is not observed, instead top edge inwards rolling in the early stage and then sidewall horizontal buckling towards centre of each unit cell are observed under 20 m/s crushing speed. This damage mode of TSP foldcore with simple boundary under dynamic loading is quite similar to the foldcore with fixed boundary under quasi-static loading as shown in Figure 14. Correlated to similarity of deformation mode, the stress-strain responses under the two scenarios (i.e. 20 m/s crushing on the foldcore with simple boundary condition and quasi-static loading on the foldcore with fixed boundary condition) are also similar, with an increasing crushing resistance during plateau stage, as seen in Figure 13 and Figure 15.

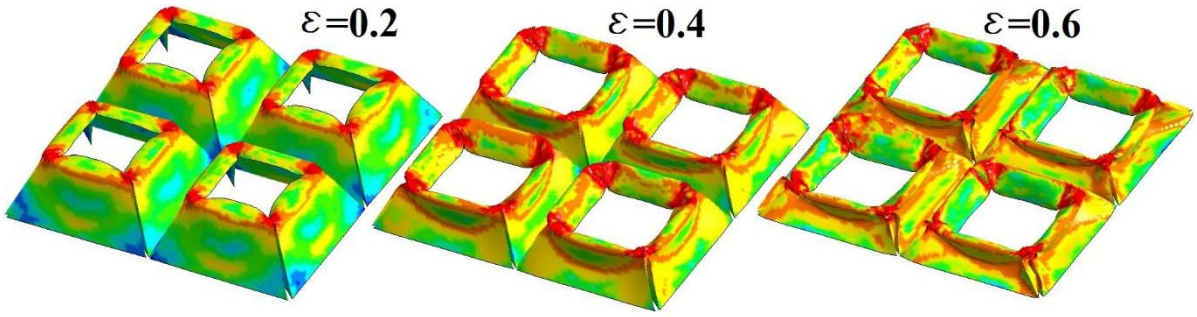

Figure 18. Damage modes of TSP folded structure with simple boundary at the strain of 0.2, 0.4 and 0.6 under 20m/s crushing

Deformation mode of TPP foldcore under 20 m/s crushing is similar to TSP under the same loading rate. The top edge of the sidewalls bends towards centre of each unit cell and further bending occurs along with further crushing of the foldcore. No sidewall buckling can be observed other than the deformation of top edges. As circled in Figure 19, slight corner open-up can be seen between two foldcores, where constraint is not provided due to the gap between tessellations of the pentagon shape. No lift-up of corner is seen for this simple boundary TPP under dynamic loading as opposed to foldcore under quasi-static crushing. Similar damage mode of the structure with simple boundary under dynamic crushing is observed as the case with fixed boundary condition under quasi-static crushing (Figure 14).

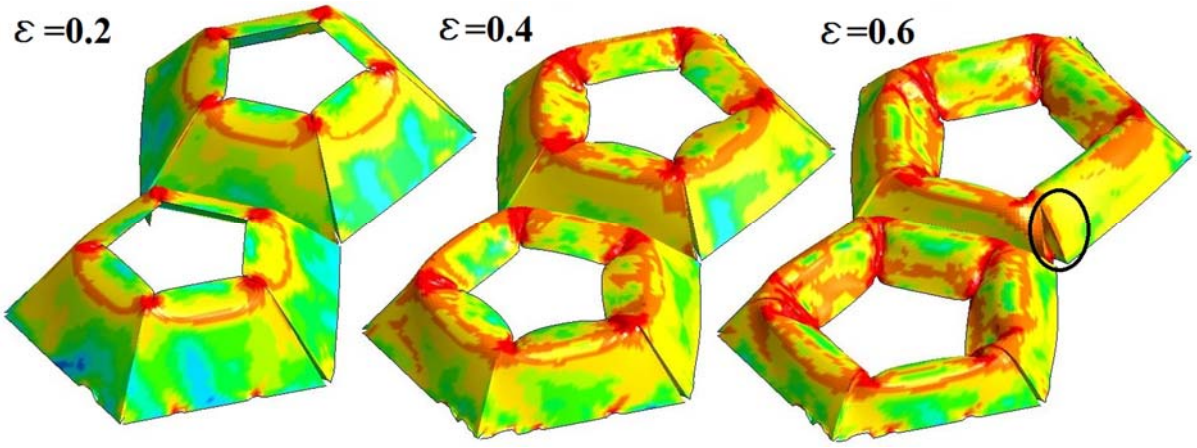

Figure 19. Damage modes of TPP folded structure with simple boundary at the strain of 0.2, 0.4 and 0.6 under 20m/s crushing

6. Conclusion

Three types of truncated pyramid folded structures (i.e. TTP, TSP and TPP) are proposed in this paper with different base shapes (i.e. triangle, square and pentagon). Quasi-static crushing experiments of the hand-folded samples with simple boundary are carried out. Numerical models of these structures are calibrated with quasi-static crushing test data and good agreement is achieved. Numerical simulations are then conducted for quasi-static and dynamic crushing of the foldcore with simple and fixed boundary conditions. The findings in this study are summarized below.

1. Under quasi-static crushing of the foldcores with simple boundary condition, superior performances of TTP and TSP are demonstrated over Miura-type foldcore with higher average crushing stress, lower initial peak and longer densification strain. TPP shows less ideal performance than TTP and TSP, because of lower inclination angle and smaller interconnection size of TPP foldcore.
2. Under quasi-static crushing of foldcores with fixed boundary condition, superior performances in terms of the key indicators, i.e., high average stress, low initial peak resistance and low uniformity ratio, are shown for all the three types of truncated folded structures as compared to Miura-type foldcore. Significant change in deformation mode and increase in crushing resistance are observed for TSP and TPP foldcores as compared to the case with simple boundary condition.
3. Under dynamic loading of the foldcores with simple boundary condition, TTP foldcore shows strain rate sensitivity with rise in initial peak stress due to the high inclination angle of sidewall. For TSP and TPP foldcores, the crushing resistances are significantly enhanced

while the initial peak stress is not significantly increased. This is caused by the change of damage mode due to inertia effect that reduces the sidewall sliding and corner lifting-up of TSP and TPP foldcores. TSP foldcore outperforms the other three types under higher loading rate, demonstrating great application potentials for energy absorption.

7. Acknowledgement

The authors acknowledge the support from Australian Research Council via Discovery Early Career Researcher Award (DE160101116).

8. References

[1] K. Miura, Zeta-core sandwich-its concept and realization, title ISAS report/Institute of Space and Aeronautical Science, University of Tokyo, 37, 1972, 137.

[2] K. Miura, Method of packaging and deployment of large membranes in space, title The Institute of Space and Astronautical Science report, 618, 1985, 1.

[3] S. Heimbs, P. Middendorf, S. Kilchert, A.F. Johnson, M. Maier, Experimental and Numerical Analysis of Composite Folded Sandwich Core Structures Under Compression, Applied Composite Materials, 14, 2008, 363-377.

[4] S. Heimbs, J. Cichosz, M. Klaus, S. Kilchert, A.F. Johnson, Sandwich structures with textile-reinforced composite foldcores under impact loads, Composite Structures, 92, 2010, 1485-1497.

[5] S. Heimbs, Foldcore sandwich structures and their impact behaviour: an overview, in: Dynamic failure of composite and sandwich structures, Springer, 2013, pp. 491-544.

[6] S. Liu, G. Lu, Y. Chen, Y.W. Leong, Deformation of the Miura-ori patterned sheet, International Journal of Mechanical Sciences, 99, 2015, 130-142.

[7] J.M. Gattas, Z. You, Quasi-static impact of indented foldcores, International Journal of Impact Engineering, 73, 2014, 15-29.

[8] J.M. Gattas, Z. You, Miura-Base Rigid Origami: Parametrizations of Curved-Crease Geometries, Journal of Mechanical Design, 136, 2014, 121404-121404-121410.

[9] J.M. Gattas, Z. You, The behaviour of curved-crease foldcores under low-velocity impact loads, International Journal of Solids and Structures, 53, 2015, 80-91.

[10] R.K. Fathers, J.M. Gattas, Z. You, Quasi-static crushing of eggbox, cube, and modified cube foldcore sandwich structures, International Journal of Mechanical Sciences, 101-102, 2015, 421-428.

[11] T. Nojima, K. Saito, Development of newly designed ultra-light core structures, JSME International Journal Series A Solid Mechanics and Material Engineering, 49, 2006, 38-42.

[12] Z. Xue, J.W. Hutchinson, Crush dynamics of square honeycomb sandwich cores, International Journal for Numerical Methods in Engineering, 65, 2006, 2221-2245.

[13] Z. Li, W. Chen, H. Hao, Numerical study of folded dome shape aluminium structure against flatwise crushing, in: 12th International Conference on Shock & Impact Loads on Structures, Singapore, 2017.

553 [14] Z. Li, W. Chen, H. Hao, Crushing behaviours of folded kirigami structure with square
554 dome shape, International Journal of Impact Engineering, 115, 2018, 94-105.

555 [15] Z. Li, W. Chen, H. Hao, Blast resistant performance of multi-layer square dome shape
556 kirigami folded structure,, in: 6th International Conference on Design and Analysis of
557 Protective Structures, Melbourne, Australia, 2017.

558 [16] H. Hao, Z. Li, W. Chen, Performance of sandwich panel with square dome shape folded
559 kirigami core under blast loading, in: 13th International Conference on Steel, Space and
560 Composite Structures, Perth, Australia, 2018.

561 [17] D.L. Caspar, E. Fontano, Five-fold symmetry in crystalline quasicrystal lattices,
562 Proceedings of the National Academy of Sciences, 93, 1996, 14271-14278.

563 [18] ASTM, E8M-04 Standard Test Methods for Tension Testing of Metallic Materials (Metric)
564 1, ASTM international, 2004.

565 [19] F. Zhu, L. Zhao, G. Lu, Z. Wang, Structural response and energy absorption of sandwich
566 panels with an aluminium foam core under blast loading, Advances in Structural Engineering,
567 11, 2008, 525-536.

568 [20] M. Abbasi, S. Reddy, A. Ghafari-Nazari, M. Fard, Multiobjective crashworthiness
569 optimization of multi-cornered thin-walled sheet metal members, Thin-Walled Structures, 89,
570 2015, 31-41.

571 [21] X. Zhou, H. Wang, Z. You, Mechanical properties of Miura-based folded cores under
572 quasi-static loads, Thin-Walled Structures, 82, 2014, 296-310.

573 [22] K. Yang, S. Xu, J. Shen, S. Zhou, Y.M. Xie, Energy absorption of thin-walled tubes with
574 pre-folded origami patterns: Numerical simulation and experimental verification, Thin-Walled
575 Structures, 103, 2016, 33-44.

576 [23] A. Pydah, R.C. Batra, Crush dynamics and transient deformations of elastic-plastic Miura-
577 ori core sandwich plates, Thin-Walled Structures, 115, 2017, 311-322.

578 [24] D.D. Radford, G.J. McShane, V.S. Deshpande, N.A. Fleck, Dynamic Compressive
579 Response of Stainless-Steel Square Honeycombs, Journal of Applied Mechanics, 74, 2007, 658.

580